Volume 11, Number 6 (December 2018) p. 1258 – 1283 • ISSN 1983-4195
http://dx.doi.org/10.1590/S1983-41952018000600006

REVISTA IBRACON DE ESTRUTURAS E MATERIAIS
IBRACON STRUCTURES AND MATERIALS JOURNAL

Reinforcement design of concrete sections based on the arc-length method

Dimensionamento de seções de concreto armado baseado no processo do arco cilíndrico


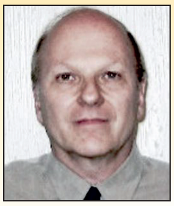

J. N. KABENJABU [a]
joelkabenjabu@id.uff.br

M. SCHULZ [a]
mschulz@id.uff.br

Abstract

The reinforcement design of concrete cross-sections with the parabola-rectangle diagram is a well-established model. A global limit analysis, considering geometrical and material nonlinear behavior, demands a constitutive relationship that better describes concrete behavior. The Sargin curve from the CEB-FIP model code, which is defined from the modulus of elasticity at the origin and the peak point, represents the descending branch of the stress-strain relationship. This research presents a numerical method for the reinforcement design of concrete cross-sections based on the arc length process. This method is numerically efficient in the descending branch of the Sargin curve, where other processes present convergence problems. The examples discuss the reinforcement design of concrete sections based on the parabola-rectangle diagram and the Sargin curve using the design parameters of the local and global models, respectively.

Keywords: reinforced concrete, design of concrete cross-sections, Sargin curve, arc-length method.

Resumo

O dimensionamento de seções transversais de concreto com o diagrama parábola-retângulo é um modelo de cálculo consagrado. A análise limite global, considerando a não linearidade física e geométrica, demanda uma relação constitutiva que descreva melhor o comportamento do concreto. A curva de Sargin do Código Modelo CEB-FIP, que é definida a partir do módulo de elasticidade na origem e do ponto de pico, representa o ramo descendente da relação tensão-deformação. Esta pesquisa apresenta um método numérico de dimensionamento de seções transversais baseado no processo do arco-cilíndrico. Este método é numericamente eficiente no ramo descendente da curva de Sargin, onde outros processos mostram problemas de convergência. Os exemplos discutem o dimensionamento de seções transversais com o diagrama parábola-retângulo e a curva de Sargin, utilizando os parâmetros de cálculo dos modelos local e global, respectivamente.

Palavras-chave: concreto armado, dimensionamento de seções de concreto, curva de Sargin, processo do arco-cilíndrico.

[a] *Fluminense Federal University, Department of Civil Engineering, Niterói, RJ, Brazil.*

Received: 19 Apr 2017 • Accepted: 12 Jun 2018 • Available Online: 23 Nov 2018

1. Introduction

Different constitutive relations have been used for the reinforcement design of concrete beams and columns. Mörsch [1] considered linear-elastic material behavior in allowable stress design. Several authors contributed to the flexural model that is nowadays used in ultimate limit state design. In the 1950s, Bernoulli's plane section hypothesis, equilibrium conditions, and nonlinear constitutive relationships for concrete and steel provided the basis for the development of reinforcement design theories. The literature review on concrete stress distribution presented by Hognestad [2] includes the contributions of Whitney [3] and Bittner [4] for rectangular and parabola-rectangle diagrams, respectively.

Simplified theories for ultimate strength under combined bending and normal force were consolidated in the early 1960s using approximate constitutive relations for concrete without any significant loss of precision. Mattock, Kriz, and Hognestad [5] adopted the rectangular diagram, while Rüsch, Grasser, and Rao [6] used the parabola-rectangle diagram.

Concrete stress distribution is currently approximated by a rectangular stress block in ACI 318-14 [7]. CEN Eurocode 2: 2004 [8], FIB Model Code 2010 [9], and ABNT NBR 6118: 2014 [10] all use the parabola-rectangle diagram.

Such simplified stress diagrams require limiting strain states for reinforcing steel and concrete to ensure valid results under combined axial and bending effects. The approximated diagrams simplify numerical design procedures and design graphs, but do not represent the characteristics of concrete, such as the initial modulus of elasticity and the descending branch of the stress-strain relationship.

Physical and geometric nonlinear analyses of reinforced concrete framed structures require stress-strain relationships that better describe the behavior of concrete. The Sargin model [11] represents several characteristics of the uniaxial behavior of concrete. The Sargin curve presented in the CEB-FIP Model Code 1990 [12] is defined by the initial modulus of elasticity, minimum compression stress, and critical strain. This curve also represents the descending branch of the stress-strain relationship.

The convergence of the Newton-Raphson method is not stable in descending branches of stress-strain curves. This study presents a numerical method for the reinforcement design of concrete sections under combined bending and normal forces that is suitable for the Sargin curve. It is based on the arc-length technique, which is stable for negative derivatives of the stress-strain diagram. The numerical procedure automatically identifies the strain distribution in the ultimate limit state without having to consider a variable strain limit in compression (domain 5). Concrete and steel strain limits are not required but can be included to avoid excessive deformations.

The examples given of reinforcement design apply both the parabola-rectangle and the Sargin curve. Design stress-strain diagrams are based on characteristic curves and code provisions for local and global analysis.

2. Simplifying assumptions

The following assumptions are considered at the outset:

1. There is no relative displacement between the steel and the surrounding concrete (steel and concrete have the same mean strain).
2. Cross-sections remain plane after deformation (Bernoulli's hypothesis).

In the interests of simplifying the formulation, steel area is not deducted from concrete area. The influence of the type of aggregate is not discussed in the present investigation.

3. Constitutive relations

Compression stresses and strains are negative.

The constitutive stress-strain relationship of steel is defined by

$$\sigma_s = \sigma_s(\varepsilon_s) \tag{1}$$

where steel stress σ_s is a function of steel strain ε_s. The yield strength and modulus of elasticity of the steel are f_y and E_s, respectively. The corresponding yield strain ε_{sy} is:

$$\varepsilon_{sy} = \frac{f_y}{E_s} \tag{2}$$

The steel stress-strain curve is divided into three regions (Figure 1), which are respectively defined by:

$$\begin{aligned} \sigma_s &= -f_y + K_s E_s(\varepsilon_s + \varepsilon_{sy}) && \text{for } \varepsilon_s < -\varepsilon_{sy} \\ \sigma_s &= E_s \varepsilon_s && \text{for } -\varepsilon_{sy} < \varepsilon_s < \varepsilon_{sy} \\ \sigma_s &= f_y + K_s E_s(\varepsilon_s - \varepsilon_{sy}) && \text{for } \varepsilon_s > \varepsilon_{sy} \end{aligned} \tag{3}$$

The convergence of the Newton-Raphson process in the yielding range is stabilized by the reduced tangent modulus $K_s E_s$. The arc-length method uses K_s=0. The steel tangent modulus $E_s(\varepsilon_s)$ is defined by the derivative:

$$E_s(\varepsilon_s) = \frac{\partial \sigma_s}{\partial \varepsilon_s} \tag{4}$$

Expressions and yield:

$$\begin{aligned} E_s(\varepsilon_s) &= K_s E_s && \text{for } \varepsilon_s < -\varepsilon_{sy} \\ E_s(\varepsilon_s) &= E_s && \text{for } -\varepsilon_{sy} < \varepsilon_s < \varepsilon_{sy} \\ E_s(\varepsilon_s) &= K_s E_s && \text{for } \varepsilon_s > \varepsilon_{sy} \end{aligned} \tag{5}$$

Concrete stress σ_c is a function of concrete strain ε_c, i.e.,

$$\sigma_c = \sigma_c(\varepsilon_c) \tag{6}$$

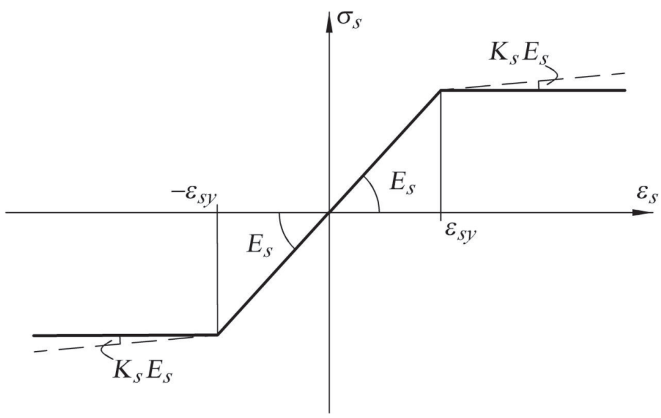

Figure 1
Stress-strain relationship of steel

CEB-FIP Model Code 1990 [12] defines the Sargin curve from the minimum compression stress σ_{c1}, the critical strain ε_{c1}, and the initial modulus of elasticity E_{c0} (Figure 2). Concrete stress is defined by:

$$\begin{aligned} &\sigma_c = \sigma_{c1}\frac{1}{b\eta^2+c\eta} && \text{for } \varepsilon_c \le \varepsilon_{c\,lim} \\ &\sigma_c = \sigma_{c1}\frac{k_1\eta-\eta^2}{(k_1-2)\eta+1} && \text{for } \varepsilon_{c\,lim} \le \varepsilon_c \le 0 \\ &\sigma_c = 0 && \text{for } 0 \le \varepsilon_c \end{aligned} \tag{7}$$

where $\varepsilon_{c\,lim}$ is the strain that separates the first two branches of the curve. The secant modulus of elasticity E_{c1} at the critical point is:

$$E_{c1} = \frac{\sigma_{c1}}{\varepsilon_{c1}} \tag{8}$$

Coefficient k_1 , variable η, and strain limit $\varepsilon_{c\,lim}$ are respectively defined by:

$$k_1 = \frac{E_{c0}}{E_{c1}} \tag{9}$$

$$\eta = \frac{\varepsilon_c}{\varepsilon_{c1}} \tag{10}$$

$$\varepsilon_{c\,lim} = \eta_{lim}\,\varepsilon_{c1} \tag{11}$$

where

$$\eta_{lim} = k_2 + \sqrt{{k_2}^2 - \frac{1}{2}} \tag{12}$$

$$k_2 = \frac{1}{2}\left(\frac{k_1}{2}+1\right) \tag{13}$$

Parameters b and c of equation (7) are respectively expressed by:

$$b = \frac{\xi_{lim}}{\eta_{lim}} - \frac{2}{\eta_{lim}^2} \tag{14}$$

$$c = \frac{4}{\eta_{lim}} - \xi_{lim} \tag{15}$$

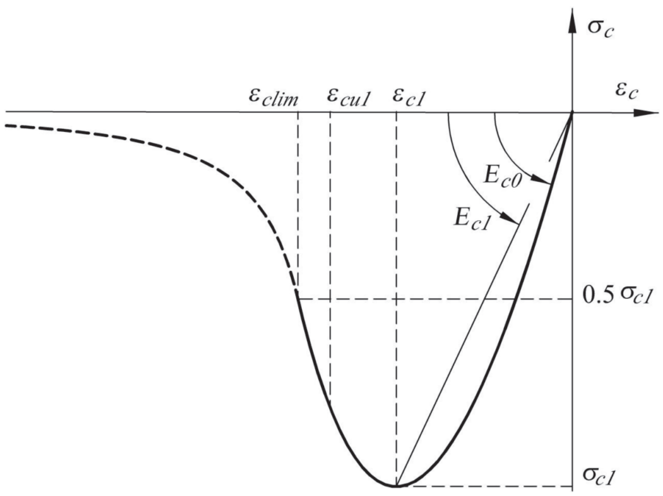

Figure 2
Stress-strain relationship of concrete

where

$$\xi_{lim} = \frac{4\left[(k_1-2)\eta_{lim}^2 + 2\eta_{lim} - k_1\right]}{\left[(k_1-2)\eta_{lim}+1\right]^2} \tag{16}$$

The tangent modulus of elasticity of concrete, $E_c\,(\varepsilon_c)$, is defined by the derivative:

$$E_c(\varepsilon_c) = \frac{\partial\sigma_c}{\partial\varepsilon_c} \tag{17}$$

Expressions and yield:

$$\begin{aligned} &E_c(\varepsilon_c) = E_{c1}\frac{(c+2b\eta)}{(b\eta^2+c\eta)^2} && \text{for } \varepsilon_c \le \varepsilon_{c\,lim} \\ &E_c(\varepsilon_c) = E_{c1}\frac{[\eta^2(2-k_1)+k_1-2\eta]}{[(k_1-2)\eta+1]^2} && \text{for } \varepsilon_{c\,lim} \le \varepsilon_c \le 0 \\ &E_c(\varepsilon_c) = 0 && \text{for } 0 \le \varepsilon_c \end{aligned} \tag{18}$$

The initial modulus of elasticity can be ascertained from equations and , i.e.,

$$E_c(0) = E_{c1}k_1 = E_{c0} \tag{19}$$

The provisions of item 5.8.6 from CEN Eurocode 2:2004 [8] are also considered. The critical strain and initial elasticity modulus are, respectively,

$$\varepsilon_{c1} = -0.7{f_{cm}}^{0.31}/1000 \ge -0.0028 \quad , \quad f_{cm}[\text{MPa}] \tag{20}$$

$$E_{c0} = (1.05)\,(22000)\,\left(f_{cm}/10\right)^{0.3}/\gamma_{cE} \quad , \quad E_{c0}, f_{cm}[\text{MPa}] \tag{21}$$

The partial factor for the elasticity modulus of concrete is γ_{cE} =1.2 and the effect of the aggregate type is not discussed in this investigation. The mean compressive strength of the concrete is estimated by $f_{cm} = f_{ck} + 8$ MPa, where f_{ck} is the characteristic compressive strength of concrete.

The partial safety factors for concrete and steel are γ_c = 1.4 and γ_s=1.15, respectively, as recommended in ABNT NBR 6118:2014 [10]. The effect of long-term sustained loads on the ultimate strength of concrete (Rüsch [13]) is considered by using α_c = 0.85 in:

$$\sigma_{c1} = -\alpha_c f_{ck}/\gamma_c \tag{22}$$

The reinforcement design examples apply both the Sargin and the parabola-rectangle curve. The reinforcement design with the parabola-rectangle diagram assumes the constitutive relation, the limit strains, and the ultimate limit-state domains provided in ABNT NBR 6118:2014 [10].

The numerical procedure proposed for the Sargin curve automatically identifies the strain distribution in the ultimate limit state without having to consider a variable strain limit in compression (domain 5). Concrete and steel strain limits are not required, but they are included to avoid excessive deformations. Steel strain is limited by:

$$\varepsilon_s \le 0.010 \tag{23}$$

Concrete strain is limited by:

$$\varepsilon_c \ge \varepsilon_{cu1} \tag{24}$$

CEN Eurocode 2:2004 [8] provides the following expression:

$$\varepsilon_{cu1} = -0.0028 - 0.027\left(\left(98-f_{cm}\right)/100\right)^4 \ge -0.0035 \quad , \quad f_{cm}[\text{MPa}] \tag{25}$$

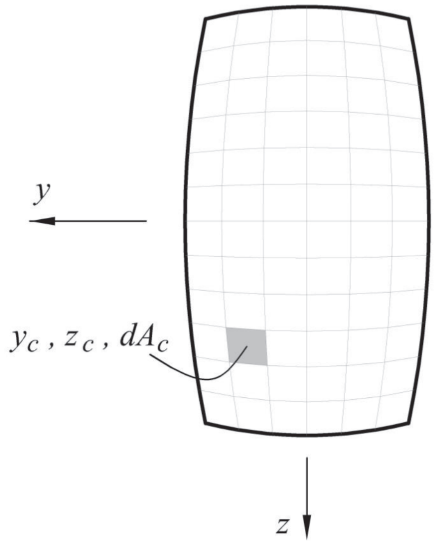

Figure 3
Cross-section

Since $\varepsilon_{c\,u1} > \varepsilon_{c\,lim}$ (Figure 2), the branch of the Sargin curve defined by $\varepsilon_c \leq \varepsilon_{c\,lim}$ is not used in the reinforcement design.

4. Equilibrium and compatibility equations

Figure 3 shows the coordinate system of the cross-section. The concrete section is discretized into area elements dA_c. The position of each element centroid is defined by the coordinates y_c and z_c. The position of each steel reinforcing bar, whose area is denoted as A_s, is defined by the coordinates y_s and z_s (Figure 4). The stress resultants are presented in Figure 5. Positive normal forces N_x are tension forces. Positive bending moments M_y and M_z correspond to tension stresses at the positive y and z faces, respectively.

According to assumption 1, there is no slip between the steel and the surrounding concrete. Concrete and steel strains, which are respectively denoted as ε_c and ε_s, have the same value, i.e.,

$$\varepsilon_c = \varepsilon_s = \varepsilon \tag{26}$$

where ε is the strain at a point in the cross-section.

Cross-sections remain plane after deformation (assumption 2). Strain ε at a point is expressed as:

$$\varepsilon = k_x + k_y y + k_z z \tag{27}$$

where k_x is the strain at the origin. Parameters k_y and k_z are the curvatures with inverted signs. The compatibility equation (27) is rewritten as:

$$\varepsilon = \mathbf{p}^T\mathbf{k} \tag{28}$$

where $p=[1\ y\ z]^T$ is a position vector and $k=[k_x\ k_y\ k_z]^T$ is the generalized strain vector.

The following expressions are obtained from the equilibrium conditions of the cross section:

$$N_x = \int_A \sigma_c dA_c + \sum \sigma_s A_s \tag{29}$$

$$M_y = \int_A \sigma_c y_c dA_c + \sum \sigma_s y_s A_s \tag{30}$$

$$M_z = \int_A \sigma_c z_c dA_c + \sum \sigma_s z_s A_s \tag{31}$$

The equilibrium equations (29), (30), and (31) are rewritten as:

$$\mathbf{S} = \int_A \mathbf{p}\sigma(\varepsilon) dA \tag{32}$$

where $\sigma(\varepsilon)$ is the stress at a point and $S = [N_x\ M_y\ M_z]^T$ is the stress resultant vector. The following incremental equation is obtained from (32):

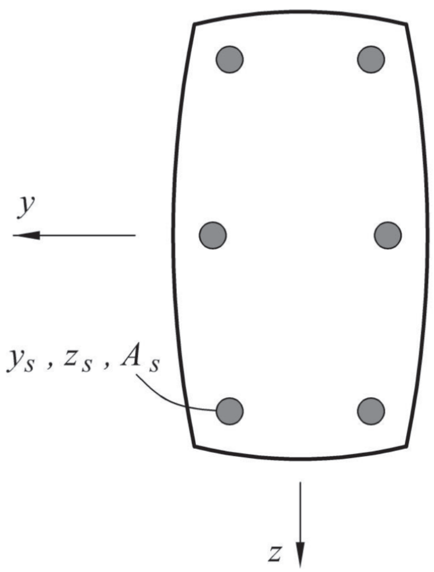

Figure 4
Steel reinforcing bars

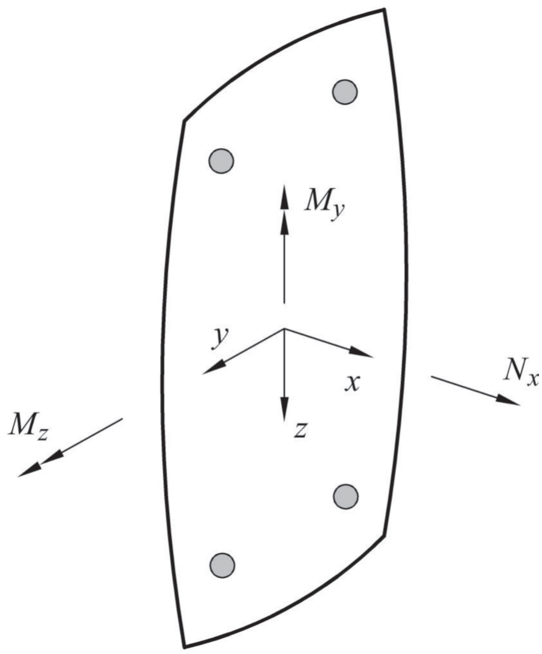

Figure 5
Stress resultants

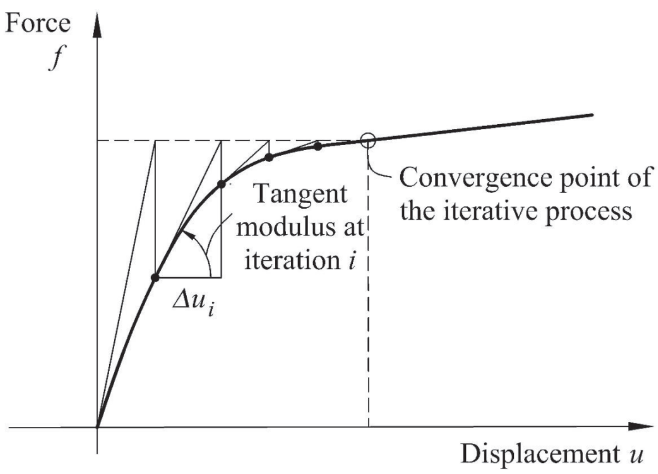

Figure 6
Newton-Raphson method

$$\Delta \mathbf{S} = \int_A \mathbf{p}\ \Delta\sigma(\varepsilon) dA = \int_A \mathbf{p}\ E(\varepsilon)\ \Delta\varepsilon\ dA \tag{33}$$

$E(\varepsilon)$ is the tangent modulus of elasticity at a point. The substitution of (28) into (33) yields:

$$\Delta \mathbf{S} = \mathbf{E}\,\Delta \mathbf{k} \tag{34}$$

where the tangent matrix E is expressed by:

$$\mathbf{E} = \int_A \mathbf{p}\ E(\varepsilon)\ \mathbf{p}^T\ dA \tag{35}$$

5. Numerical methods for section analysis and reinforcement design

Figure 6 shows the solution for a nonlinear structural system of a single degree of freedom based on the Newton-Raphson process. The arc-length process is a variant of the Newton-Raphson method that controls the progress of the iterative process (Figure 7). The arc-length and load factor are denoted as l and λ, respectively. The incremental process is capable of passing through critical points.

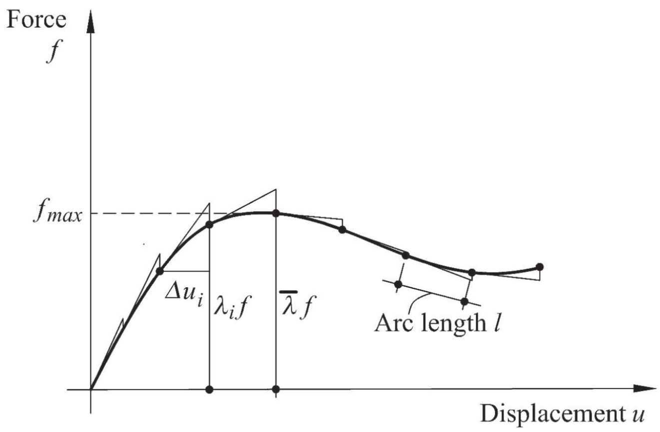

Figure 7
Arc-length method

The section analysis and reinforcement design methods are applicable, but not limited, to the Sargin stress-strain relationship.

5.1 Arc-length method

The arc-length method presented by Crisfield [14] is an alternative formulation of the method originally proposed by Riks [15].
The stress resultant vector is defined as $\lambda\bar{\mathbf{S}}$, where λ is a load factor and $\bar{\mathbf{S}} = [\bar{N}_x \quad \bar{M}_y \quad \bar{M}_z]$ is the stress resultant vector that is established as a reference.
The term ΔS_i is defined as:

$$\Delta \mathbf{S}_i = \lambda\bar{\mathbf{S}} - \mathbf{S}_i \tag{36}$$

where $S_i = [N_{x,i}\ M_{y,i}\ M_{z,i}]$ is the stress resultant vector associated with the generalized strain vector $k_i = [k_{x,i}\ k_{y,i}\ k_{z,i}]^T$ at iteration i.
Equation is rewritten as:

$$\Delta \mathbf{k}_i = \mathbf{E}_i^{-1}\Delta \mathbf{S}_i \tag{37}$$

where E_i is a tangent matrix and Δk_i is the increment of the generalized strain vector at iteration i. Equations (36) and (37) yield:

$$\Delta \mathbf{k}_i = \lambda \mathbf{E}_i^{-1}\bar{\mathbf{S}} - \mathbf{E}_i^{-1}\mathbf{S}_i = \lambda\bar{\mathbf{g}}_i - \mathbf{g}_i \tag{38}$$

where

$$\bar{\mathbf{g}}_i = \mathbf{E}_i^{-1}\bar{\mathbf{S}} \tag{39}$$

$$l^2 = \Delta\mathbf{k}_i^T \Delta\mathbf{k}_i \tag{40}$$

The arc-length l is expressed by:

$$l^2 = \Delta\mathbf{k}_i^T \Delta\mathbf{k}_i \tag{41}$$

The substitution of (38) into (41) yields:

$$l^2 = (\lambda\bar{\mathbf{g}}_i^T - \mathbf{g}_i^T)(\lambda\bar{\mathbf{g}}_i - \mathbf{g}_i) = \lambda^2\bar{\mathbf{g}}_i^T\bar{\mathbf{g}}_i - 2\lambda\bar{\mathbf{g}}_i^T\mathbf{g}_i + \mathbf{g}_i^T\mathbf{g}_i \tag{42}$$

Expression (42) defines the quadratic equation:

$$a\lambda^2 + b\lambda + c = 0 \tag{43}$$

where

$$a = \bar{\mathbf{g}}_i^T\bar{\mathbf{g}}_i \quad ; \quad b = -2\bar{\mathbf{g}}_i^T\mathbf{g}_i \quad ; \quad c = \mathbf{g}_i^T\mathbf{g}_i - l^2 \tag{44}$$

One of the roots of equation (43) corresponds to the factor λ of the next iteration. The appropriate root is discussed in the next item.

5.2 Section analysis

The parameters required for section analysis are the steel and concrete properties, the geometric characteristics of the cross-section, the position and area of the reinforcing steel bars, the reference stress resultant vector $\bar{\mathbf{S}}$, and the arc-length l. The maximum load factor $\bar{\lambda}$ found throughout the incremental process defines the cross-section strength.
A brief summary of the iterative process is presented next.

I. Generalized strains k_i at iteration i

Iteration i starts with vector k_i. The first iteration can start with k_1=0.

II. Generalized stresses S_i and tangent matrix E_i

The strains $\varepsilon = p^T k_i$, stresses $\sigma(\varepsilon)$, and tangent moduli of elasticity $E(\varepsilon)$ are determined for each area element of the steel and concrete. Expressions (32) and (35) yield the generalized stresses S_i and tangent matrices E_i, respectively.

III. Load factors λ_A and λ_B

Equations (39) and (40) yield the auxiliary vectors $\bar{\mathbf{g}}_i$ and $\mathbf{g}_i$, respectively. Load factors λ_A and λ_B are the solutions of the quadratic equation established by (43) and (44).

IV. Load factor λ

The root of (43) that pushes forward the incremental process is selected. The first iteration elects $\lambda_1 = \max(\lambda_A, \lambda_B)$. For iteration i>1, equation (38) yields:

$$\Delta\mathbf{k}_A = \lambda_A \bar{\mathbf{g}}_i - \mathbf{g} \quad (45)$$

$$\Delta\mathbf{k}_B = \lambda_B \bar{\mathbf{g}}_i - \mathbf{g}_i \quad (46)$$

where Δk_A and Δk_B are the strain vector increments of roots λ_A and λ_B, respectively.
The slopes θ_A and θ_B of roots λ_A and λ_B are respectively defined as:

$$\theta_A = \Delta\mathbf{k}_{i-1}^T \Delta\mathbf{k}_A \quad (47)$$

$$\theta_B = \Delta\mathbf{k}_{i-1}^T \Delta\mathbf{k}_B \quad (48)$$

The load factor λ associated with the maximum slope $\theta = \max(\theta_A, \theta_B)$ is selected. The corresponding increment Δk_A or Δk_B is denoted as Δk_i. The generalized strain vector k_{i+1} of the next iteration is:

$$\mathbf{k}_{i+1} = \mathbf{k}_i + \Delta\mathbf{k}_i \quad (49)$$

The procedure returns to step II to start a new iteration. The process terminates when steel or concrete strains reach their limit values. Section strength is defined by $\bar{\lambda}\bar{\mathbf{S}}$, where $\bar{\lambda}$ is the maximum load factor found throughout the incremental process.

5.3 Reinforcement design

The parameters required for reinforcement design are the steel and concrete properties, the geometric characteristics of the cross-section, the position and relative area of each reinforcing steel bar, the minimum and maximum steel ratios, the reference stress resultant vector $\bar{S}$, and the arc-length l. The design stress resultants are defined by $\lambda_d \bar{S}$, where λ_d is the corresponding load factor.
A brief summary of the iterative process is presented next.

I. Stress analysis for minimum reinforcement

The procedure in item 5.2 yields the maximum load factor $\bar{\lambda}_{A_{s\,min}}$ for the minimum reinforcement $A_{s\,min}$. If $\lambda_d \le \bar{\lambda}_{A_{s\,min}}$, the required reinforcement is $A_{s\,min}$ and the process is terminated. Otherwise, $\lambda_{INF} = \bar{\lambda}_{A_{s\,min}}$ and $A_{s\,INF} = A_{s\,min}$.

II. Stress analysis for maximum reinforcement

The procedure in item 5.2 yields the maximum load factor $\bar{\lambda}_{A_{s\,max}}$ for the maximum reinforcement $A_{s\,max}$. If $\lambda_d > \bar{\lambda}_{A_{s\,max}}$, the cross-section is not adequate and the process is terminated. Otherwise, $\lambda_{SUP} = \bar{\lambda}_{A_{s\,max}}$ and $A_{s\,SUP} = A_{s\,max}$.

III. Iterative process

The required reinforcement is estimated by linear interpolation

$$A_s = A_{s\,INF} + (A_{s\,SUP} - A_{s\,INF}) \frac{\lambda_d - \lambda_{INF}}{\lambda_{SUP} - \lambda_{INF}} \quad (50)$$

The procedure in item 5.2 yields the maximum load factor $\bar{\lambda}$ for A_s. If $\bar{\lambda} > \lambda_d$, the new limit is defined by $\lambda_{SUP} = \bar{\lambda}$ and $A_{s\,SUP} = A_s$. Otherwise, $\lambda_{INF} = \bar{\lambda}$ and $A_{S\,INF} = A_s$.
A new iteration restarts when $A_{s\,SUP} - A_{s\,INF} > TOL_d$, where TOL_d is the tolerance for the reinforcement design. The iterative process ends when $A_{s\,SUP} - A_{s\,INF} \le TOL_d$. The required reinforcement is conservatively assumed to be $A_{s\,SUP}$. This study considers $TOL_d = 1 \times 10^{-7}$ m².

6. Examples and numerical results

The reinforcement design procedure based on the arc-length method is implemented in two Fortran programs, which use parabola-rectangle and Sargin curves, respectively. Programs Fx4 and Fx5 are presented in Kabenjabu [16].
The typical rectangular cross-section is defined by $b_y = 0.25$ m and $b_z = 0.80$ m (Figure 8). The rebar edge distances in y and z directions are $d'_y = 0.05$ m and $d'_z = 0.05$ m, respectively.
The concrete section is discretized in 25×80 area elements. The section is considered doubly reinforced in most examples, but it is also studied as singly reinforced for pure bending.
The characteristic yield strength of steel is f_{yk} = 500MPa.

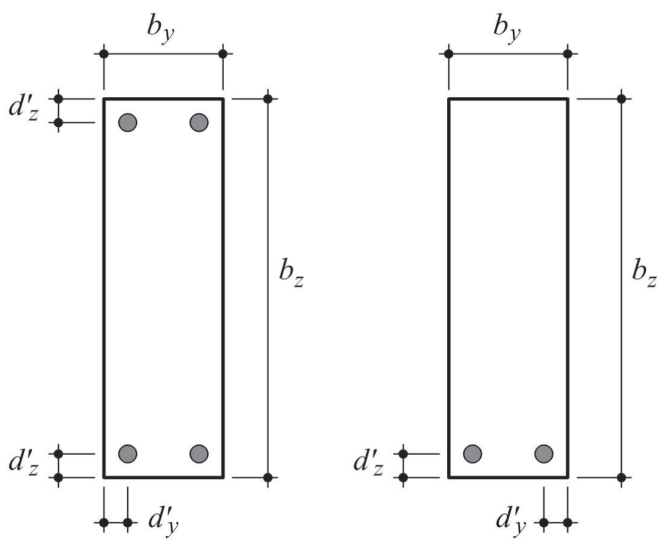

Figure 8
Typical cross-sections with and without compression reinforcement

Table 1
Doubly-reinforced cross-section subjected to pure compression

	Stress resultants			Parabola-rectangle diagram			Sargin curve			Diff.	Relative difference
	N_x (kN)	M_y (kNm)	M_z (kNm)	$A_{s\,tot}$ (cm²)	$\varepsilon_{c\,min}$	$\varepsilon_{s\,max}$	$A_{s\,tot}$ (cm²)	$\varepsilon_{c\,min}$	$\varepsilon_{s\,max}$	$\Delta A_{s\,tot}$ (cm²)	$\Delta A_{stot}/A_{stot}$
C15	-3000	0	0	28.0	-0.00200	-0.00200	27.2	-0.00207	-0.00207	-0.8	-2.9%
	-4000	0	0	51.8	-0.00200	-0.00200	50.2	-0.00207	-0.00207	-1.6	-3.1%
	-5000	0	0	75.6	-0.00200	-0.00200	73.2	-0.00207	-0.00207	-2.4	-3.2%
C30	-4000	0	0	8.5	-0.00200	-0.00200	8.2	-0.00216	-0.00216	-0.3	-3.4%
	-4500	0	0	20.4	-0.00200	-0.00200	19.7	-0.00216	-0.00216	-0.7	-3.4%
	-5000	0	0	32.3	-0.00200	-0.00200	31.2	-0.00216	-0.00216	-1.1	-3.4%
	-5500	0	0	44.2	-0.00200	-0.00200	42.7	-0.00216	-0.00216	-1.5	-3.4%
	-6000	0	0	56.1	-0.00200	-0.00200	54.2	-0.00216	-0.00216	-1.9	-3.4%
	-6500	0	0	68.0	-0.00200	-0.00200	65.7	-0.00216	-0.00216	-2.3	-3.4%
	-7000	0	0	79.9	-0.00200	-0.00200	77.2	-0.00216	-0.00216	-2.7	-3.4%
C45	-6000	0	0	12.7	-0.00200	-0.00200	12.3	-0.00240	-0.00240	-0.4	-3.3%
	-7000	0	0	36.5	-0.00200	-0.00200	35.3	-0.00240	-0.00240	-1.2	-3.3%
	-8000	0	0	60.3	-0.00200	-0.00200	58.3	-0.00240	-0.00240	-2.0	-3.3%

The examples investigate concrete grades C15, C30, and C45. The corresponding compressive strengths are 15 MPa, 30 MPa and 45MPa, respectively. Although C15 concrete is no longer in use, it is included in the study because of its widespread use in the past.

The partial safety factors for concrete and steel are γ_c = 1.4 and γ_s = 1.15, respectively, as recommended in ABNT NBR 6118:2014 [10]. N_x, M_y, and M_z are the design values of the stress resultants.

The examples are summarized in Tables 1 to 9, where $A_{s\,tot}$ is the required total reinforcement, $\varepsilon_{c\,min}$ is the minimum concrete strain, and $\varepsilon_{s\,max}$ is the maximum steel strain. The relative difference $\Delta A_{s\,tot}/A_{s\,tot}$ is defined as:

$$\Delta A_{s\,tot}/A_{s\,tot} = \left(A_{s\,tot,SARGIN} - A_{s\,tot,PAR-RECT}\right)/A_{s\,tot,PAR-RECT} \quad (51)$$

where $A_{s\,tot,PAR\text{-}RECT}$ and $A_{s\,tot,SARGIN}$ are the required total reinforcement for parabola-rectangle and Sargin curves, respectively.

The section is subjected to pure compression in Table 1. The Sargin curve yields lower reinforcement values than the parabola-rectangle diagram. The limit strain ε_{cu2} = -0.002 of the parabola-rectangle

Table 2
Doubly-reinforced cross-section subjected to compression and uniaxial bending ($e_z = b_z/4$)

	Stress resultants			Parabola-rectangle diagram			Sargin curve			Diff.	Relative difference
	N_x (kN)	M_y (kNm)	M_z (kNm)	$A_{s\,tot}$ (cm²)	$\varepsilon_{c\,min}$	$\varepsilon_{s\,max}$	$A_{s\,tot}$ (cm²)	$\varepsilon_{c\,min}$	$\varepsilon_{s\,max}$	$\Delta A_{s\,tot}$ (cm²)	$\Delta A_{stot}/A_{stot}$
C15	-1250	0	250	8.3	-0.00350	0.00077	8.4	-0.00295	0.00085	0.1	1.3%
	-1750	0	350	24.4	-0.00350	0.00027	24.3	-0.00284	0.00034	0.0	0.0%
	-2250	0	450	41.7	-0.00350	0.00005	41.6	-0.00275	0.00012	-0.1	-0.2%
	-2750	0	550	59.4	-0.00345	-0.00008	59.2	-0.00270	-0.00001	-0.2	-0.3%
	-3250	0	650	77.3	-0.00339	-0.00016	77.1	-0.00266	-0.00009	-0.2	-0.3%
C30	-2250	0	450	9.7	-0.00350	0.00103	10.7	-0.00318	0.00100	1.0	**10.1%**
	-2500	0	500	16.6	-0.00350	0.00077	17.7	-0.00318	0.00077	1.1	**6.5%**
	-2750	0	550	24.2	-0.00350	0.00059	25.3	-0.00317	0.00059	1.1	4.6%
	-3000	0	600	32.1	-0.00350	0.00045	33.2	-0.00315	0.00046	1.1	3.6%
	-3250	0	650	40.3	-0.00350	0.00035	41.5	-0.00313	0.00036	1.2	2.9%
	-3500	0	700	48.7	-0.00350	0.00027	49.9	-0.00311	0.00028	1.2	2.4%
	-3750	0	750	57.2	-0.00350	0.00020	58.4	-0.00309	0.00021	1.2	2.0%
	-4000	0	800	65.9	-0.00351	0.00014	67.0	-0.00308	0.00015	1.2	1.8%
C45	-3250	0	650	11.4	-0.00350	0.00115	13.5	-0.00338	0.00105	2.1	**18.2%**
	-3500	0	700	17.9	-0.00350	0.00093	20.2	-0.00339	0.00086	2.3	**13.0%**
	-4000	0	800	32.4	-0.00350	0.00064	35.0	-0.00338	0.00059	2.7	**8.2%**
	-4500	0	900	48.2	-0.00350	0.00045	51.0	-0.00336	0.00041	2.8	**5.9%**
	-5000	0	1000	64.6	-0.00350	0.00032	67.6	-0.00334	0.00029	3.0	4.6%

Table 3
Doubly-reinforced cross-section subjected to compression and uniaxial bending ($e_z = b_z/2$)

	Stress resultants			Parabola-rectangle diagram			Sargin curve			Diff.	Relative difference
	N_x (kN)	M_y (kNm)	M_z (kNm)	$A_{s\,tot}$ (cm²)	$\varepsilon_{c\,min}$	$\varepsilon_{s\,max}$	$A_{s\,tot}$ (cm²)	$\varepsilon_{c\,min}$	$\varepsilon_{s\,max}$	$\Delta A_{s\,tot}$ (cm²)	$\Delta A_{stot}/A_{stot}$
C15	-750	0	300	8.3	-0.00350	0.00301	8.4	-0.00259	0.00244	0.1	0.7%
	-1000	0	400	16.1	-0.00350	0.00170	15.9	-0.00350	0.00188	-0.3	-1.6%
	-1250	0	500	26.7	-0.00351	0.00126	26.5	-0.00350	0.00140	-0.3	-1.0%
	-1500	0	600	38.0	-0.00350	0.00101	37.8	-0.00344	0.00112	-0.3	-0.7%
	-1750	0	700	49.7	-0.00350	0.00085	49.5	-0.00336	0.00094	-0.2	-0.5%
	-2000	0	800	61.6	-0.00350	0.00075	61.3	-0.00329	0.00081	-0.2	-0.4%
C30	-1000	0	400	7.4	-0.00350	0.00634	7.6	-0.00287	0.00515	0.1	1.9%
	-1250	0	500	11.6	-0.00350	0.00434	11.8	-0.00290	0.00355	0.2	1.9%
	-1500	0	600	16.7	-0.00350	0.00301	17.0	-0.00291	0.00248	0.3	1.9%
	-1750	0	700	22.7	-0.00350	0.00207	23.3	-0.00337	0.00207	0.6	2.7%
	-2000	0	800	32.2	-0.00350	0.00170	32.8	-0.00350	0.00175	0.5	1.7%
	-2250	0	900	42.6	-0.00350	0.00144	43.2	-0.00350	0.00149	0.6	1.5%
	-2500	0	1000	53.4	-0.00351	0.00126	54.1	-0.00351	0.00130	0.7	1.3%
	-2750	0	1100	64.6	-0.00350	0.00112	65.4	-0.00350	0.00116	0.7	1.1%
C45	-1500	0	600	11.1	-0.00350	0.00634	11.4	-0.00312	0.00532	0.3	2.8%
	-2000	0	800	19.8	-0.00350	0.00384	20.3	-0.00312	0.00317	0.6	2.8%
	-2500	0	1000	30.9	-0.00350	0.00235	31.8	-0.00331	0.00207	0.9	2.9%
	-3000	0	1200	48.4	-0.00350	0.00170	50.3	-0.00350	0.00166	1.9	4.0%
	-3500	0	1400	69.2	-0.00350	0.00137	71.4	-0.00351	0.00135	2.2	3.2%

diagram is smaller in modulus than the design value of the yield strain of the steel (ε_{syd} = 0.00207). Steel stresses are higher with the Sargin curve since they reach the yield point. The differences between the two models are small and less than 5% in required reinforcement.
Tables 2 and 3 consider combined compression and uniaxial bending with eccentricities of $e_z = b_z/4$ and $e_z = b_z/2$, respectively, where $e_z = |M_z/N_x|$. In Table 4, the section is subjected to compression and biaxial bending with $e_y = b_y/4$ and $e_z = b_z/4$, where $e_y = |M_y/N_x|$. Table 5 discusses compression and biaxial bending with $e_y = b_y/2$ and $e_z = b_z/2$. Tables 6 and 7 consider compression and uniaxial bending with $e_y = b_y/4$ and $e_y = b_y/2$, respectively. Table 8 investigates pure bending with compression reinforcement. The relative differences are always less than 5% in Tables 3, 5, 7 and 8.

Table 4
Doubly-reinforced cross-section subjected to compression and biaxial bending ($e_y = b_y/4$ and $e_z = b_z/4$)

	Stress resultants			Parabola-rectangle diagram			Sargin curve			Diff.	Relative difference
	N_x (kN)	M_y (kNm)	M_z (kNm)	$A_{s\,tot}$ (cm²)	$\varepsilon_{c\,min}$	$\varepsilon_{s\,max}$	$A_{s\,tot}$ (cm²)	$\varepsilon_{c\,min}$	$\varepsilon_{s\,max}$	$\Delta A_{s\,tot}$ (cm²)	$\Delta A_{stot}/A_{stot}$
C15	-850	53.125	170	9.3	-0.00350	0.00185	8.4	-0.00332	0.00207	-0.8	**-9.0%**
	-1000	62.500	200	15.2	-0.00350	0.00158	13.9	-0.00350	0.00186	-1.3	**-8.6%**
	-1250	78.125	250	26.4	-0.00350	0.00131	25.0	-0.00350	0.00152	-1.4	**-5.4%**
	-1500	93.750	300	38.3	-0.00350	0.00115	36.8	-0.00350	0.00131	-1.4	-3.7%
	-1750	109.375	350	50.5	-0.00350	0.00105	49.1	-0.00350	0.00118	-1.4	-2.7%
	-2000	125.000	400	62.8	-0.00350	0.00098	61.5	-0.00350	0.00109	-1.3	-2.1%
	-2250	140.625	450	75.3	-0.00350	0.00092	74.0	-0.00350	0.00102	-1.3	-1.7%
C30	-1500	93.750	300	11.8	-0.00350	0.00211	11.8	-0.00350	0.00229	0.0	0.2%
	-1750	109.375	350	20.4	-0.00350	0.00180	19.8	-0.00350	0.00193	-0.6	-3.0%
	-2000	125.000	400	30.5	-0.00350	0.00158	29.8	-0.00350	0.00170	-0.7	-2.4%
	-2250	140.625	450	41.4	-0.00350	0.00143	40.6	-0.00350	0.00152	-0.7	-1.8%
	-2500	156.250	500	52.8	-0.00350	0.00131	52.1	-0.00350	0.00140	-0.7	-1.4%
	-2750	171.875	550	64.5	-0.00350	0.00122	63.8	-0.00350	0.00130	-0.7	-1.1%
C45	-2000	125.000	400	11.1	-0.00350	0.00243	11.9	-0.00350	0.00242	0.8	**7.3%**
	-2250	140.625	450	17.6	-0.00350	0.00211	18.6	-0.00350	0.00210	1.0	**5.4%**
	-2500	156.250	500	26.0	-0.00350	0.00189	27.1	-0.00350	0.00188	1.2	4.5%
	-2750	171.875	550	35.5	-0.00350	0.00172	36.8	-0.00350	0.00171	1.3	3.7%
	-3000	187.500	600	45.7	-0.00350	0.00158	47.2	-0.00350	0.00158	1.4	3.2%
	-3250	203.125	650	56.5	-0.00350	0.00147	58.1	-0.00350	0.00147	1.6	2.8%
	-3500	218.750	700	67.7	-0.00350	0.00139	69.3	-0.00350	0.00138	1.7	2.5%

Table 5
Doubly-reinforced cross-section subjected to compression and biaxial bending ($e_y = b_y/2$ and $e_z = b_z/2$)

	Stress resultants			Parabola-rectangle diagram			Sargin curve			Diff.	Relative difference
	N_x (kN)	M_y (kNm)	M_z (kNm)	$A_{s\,tot}$ (cm^2)	$\varepsilon_{c\,min}$	$\varepsilon_{s\,max}$	$A_{s\,tot}$ (cm^2)	$\varepsilon_{c\,min}$	$\varepsilon_{s\,max}$	$\Delta A_{s\,tot}$ (cm^2)	$\Delta A_{stot}/A_{stot}$
C15	-400	50	160	10.3	-0.00350	0.00364	9.8	-0.00350	0.00407	-0.5	-4.8%
	-600	75	240	21.2	-0.00350	0.00268	20.6	-0.00350	0.00300	-0.6	-2.7%
	-800	100	320	33.2	-0.00350	0.00216	32.7	-0.00337	0.00232	-0.5	-1.5%
	-1000	125	400	47.6	-0.00350	0.00191	45.6	-0.00350	0.00205	-2.0	-4.3%
	-1200	150	480	63.1	-0.00350	0.00177	61.0	-0.00350	0.00189	-2.1	-3.3%
C30	-600	75	240	11.7	-0.00350	0.00456	11.4	-0.00350	0.00477	-0.2	-2.0%
	-800	100	320	20.7	-0.00350	0.00364	20.4	-0.00350	0.00381	-0.3	-1.4%
	-1000	125	400	31.0	-0.00350	0.00308	30.8	-0.00350	0.00323	-0.3	-0.9%
	-1200	150	480	42.3	-0.00350	0.00268	42.0	-0.00350	0.00281	-0.3	-0.6%
	-1400	175	560	54.1	-0.00350	0.00239	53.9	-0.00350	0.00251	-0.2	-0.4%
	-1600	200	640	66.3	-0.00350	0.00216	66.2	-0.00350	0.00226	-0.1	-0.2%
C45	-600	75	240	7.5	-0.00350	0.00634	7.6	-0.00350	0.00630	0.1	1.8%
	-800	100	320	13.6	-0.00350	0.00500	13.9	-0.00350	0.00498	0.3	1.9%
	-1000	125	400	21.7	-0.00350	0.00419	22.1	-0.00350	0.00417	0.4	1.8%
	-1200	150	480	31.0	-0.00350	0.00364	31.5	-0.00350	0.00363	0.5	1.6%
	-1400	175	560	41.2	-0.00350	0.00324	41.8	-0.00350	0.00323	0.6	1.4%
	-1600	200	640	52.1	-0.00350	0.00293	52.8	-0.00350	0.00292	0.7	1.3%
	-1800	225	720	63.5	-0.00350	0.00268	64.2	-0.00350	0.00267	0.8	1.2%

Table 6
Doubly-reinforced cross-section subjected to compression and uniaxial bending ($e_y = b_y/4$)

	Stress resultants			Parabola-rectangle diagram			Sargin curve			Diff.	Relative difference
	N_x (kN)	M_y (kNm)	M_z (kNm)	$A_{s\,tot}$ (cm^2)	$\varepsilon_{c\,min}$	$\varepsilon_{s\,max}$	$A_{s\,tot}$ (cm^2)	$\varepsilon_{c\,min}$	$\varepsilon_{s\,max}$	$\Delta A_{s\,tot}$ (cm^2)	$\Delta A_{stot}/A_{stot}$
C15	-1250	78.125	0	12.2	-0.00350	0.00048	12.3	-0.00286	0.00056	0.1	1.2%
	-1500	93.750	0	22.0	-0.00350	0.00031	22.1	-0.00280	0.00037	0.1	0.3%
	-1750	109.375	0	32.2	-0.00350	0.00021	32.2	-0.00277	0.00027	0.0	0.0%
	-2000	125.000	0	42.5	-0.00350	0.00014	42.4	-0.00275	0.00020	-0.1	-0.1%
	-2250	140.625	0	52.8	-0.00350	0.00010	52.8	-0.00274	0.00015	-0.1	-0.1%
	-2500	156.250	0	63.3	-0.00350	0.00006	63.2	-0.00273	0.00011	-0.1	-0.2%
	-2750	171.875	0	73.7	-0.00350	0.00004	73.6	-0.00272	0.00008	-0.1	-0.2%
C30	-2100	131.250	0	9.7	-0.00350	0.00075	11.0	-0.00304	0.00071	1.3	**13.9%**
	-2250	140.625	0	15.0	-0.00350	0.00063	16.4	-0.00307	0.00061	1.4	**9.3%**
	-2500	156.250	0	24.3	-0.00350	0.00048	25.7	-0.00308	0.00048	1.4	**5.9%**
	-2750	171.875	0	34.1	-0.00350	0.00038	35.5	-0.00308	0.00039	1.4	4.2%
	-3000	187.500	0	44.0	-0.00350	0.00031	45.5	-0.00307	0.00032	1.4	3.3%
	-3250	203.125	0	54.1	-0.00350	0.00025	55.5	-0.00307	0.00026	1.4	2.6%
	-3500	218.750	0	64.3	-0.00350	0.00021	65.8	-0.00306	0.00022	1.4	2.2%
	-3750	234.375	0	74.6	-0.00350	0.00017	76.0	-0.00306	0.00019	1.4	1.9%
C45	-3000	187.500	0	9.6	-0.00350	0.00086	12.4	-0.00323	0.00074	2.8	**28.7%**
	-3250	203.125	0	18.0	-0.00350	0.00069	21.1	-0.00327	0.00061	3.1	**17.0%**
	-3500	218.750	0	27.1	-0.00350	0.00057	30.3	-0.00328	0.00051	3.2	**11.9%**
	-3750	234.375	0	36.5	-0.00350	0.00048	39.8	-0.00329	0.00044	3.4	**9.2%**
	-4000	250.000	0	46.2	-0.00350	0.00041	49.6	-0.00329	0.00038	3.4	**7.4%**
	-4250	265.625	0	56.0	-0.00350	0.00036	59.5	-0.00329	0.00032	3.5	**6.2%**
	-4500	281.250	0	66.0	-0.00350	0.00031	69.6	-0.00329	0.00028	3.5	**5.3%**
	-4750	296.875	0	76.1	-0.00350	0.00027	79.7	-0.00329	0.00025	3.6	4.7%

Table 7
Doubly-reinforced cross-section subjected to compression and uniaxial bending ($e_y = b_y/2$)

	Stress resultants			Parabola-rectangle diagram			Sargin curve			Diff.	Relative difference
	N_x (kN)	M_y (kNm)	M_z (kNm)	$A_{s\,tot}$ (cm²)	$\varepsilon_{c\,min}$	$\varepsilon_{s\,max}$	$A_{s\,tot}$ (cm²)	$\varepsilon_{c\,min}$	$\varepsilon_{s\,max}$	$\Delta A_{s\,tot}$ (cm²)	$\Delta A_{stot}/A_{stot}$
C15	-750	93.75	0	12.1	-0.00350	0.00214	12.6	-0.00344	0.00248	0.4	3.4%
	-1000	125.00	0	24.9	-0.00350	0.00148	24.7	-0.00350	0.00161	-0.2	-0.9%
	-1250	156.25	0	39.1	-0.00350	0.00120	38.9	-0.00350	0.00129	-0.2	-0.6%
	-1500	187.50	0	53.8	-0.00350	0.00105	53.6	-0.00339	0.00111	-0.2	-0.5%
	-1750	218.75	0	68.7	-0.00350	0.00095	68.5	-0.00344	0.00101	-0.2	-0.3%
C30	-1000	125.00	0	11.2	-0.00350	0.00471	11.7	-0.00307	0.00399	0.5	4.4%
	-1250	156.25	0	17.1	-0.00350	0.00321	17.9	-0.00350	0.00327	0.8	4.5%
	-1500	187.50	0	24.3	-0.00350	0.00214	25.0	-0.00332	0.00207	0.7	3.1%
	-1750	218.75	0	36.4	-0.00350	0.00172	37.3	-0.00350	0.00175	0.9	2.4%
	-2000	250.00	0	49.8	-0.00350	0.00148	50.7	-0.00350	0.00151	0.9	1.8%
	-2250	281.25	0	63.9	-0.00350	0.00132	64.8	-0.00350	0.00135	1.0	1.5%
	-2500	312.50	0	78.2	-0.00350	0.00120	79.2	-0.00350	0.00123	1.0	1.3%
C45	-1250	156.25	0	11.5	-0.00350	0.00620	12.1	-0.00310	0.00510	0.5	4.4%
	-1500	187.50	0	16.8	-0.00350	0.00471	17.4	-0.00321	0.00397	0.7	4.1%
	-1750	218.75	0	22.6	-0.00350	0.00365	23.4	-0.00340	0.00333	0.9	3.8%
	-2000	250.00	0	28.9	-0.00350	0.00285	29.9	-0.00350	0.00271	1.0	3.5%
	-2250	281.25	0	36.4	-0.00350	0.00214	38.2	-0.00350	0.00205	1.7	4.8%
	-2500	312.50	0	48.2	-0.00350	0.00183	50.7	-0.00350	0.00178	2.4	5.0%
	-2750	343.75	0	61.2	-0.00350	0.00163	63.8	-0.00350	0.00159	2.6	4.2%
	-3000	375.00	0	74.7	-0.00350	0.00148	77.5	-0.00350	0.00145	2.8	3.7%

Table 8
Doubly-reinforced cross-section subjected to pure bending

	Stress resultants			Parabola-rectangle diagram			Sargin curve			Diff.	Relative difference
	N_x (kN)	M_y (kNm)	M_z (kNm)	$A_{s\,tot}$ (cm²)	$\varepsilon_{c\,min}$	$\varepsilon_{s\,max}$	$A_{s\,tot}$ (cm²)	$\varepsilon_{c\,min}$	$\varepsilon_{s\,max}$	$\Delta A_{s\,tot}$ (cm²)	$\Delta A_{stot}/A_{stot}$
C15	0	0	150	9.7	-0.00147	0.01000	9.7	-0.00130	0.01001	0.0	-0.1%
	0	0	300	19.7	-0.00189	0.01000	19.7	-0.00177	0.01000	0.0	0.2%
	0	0	450	29.6	-0.00211	0.01001	29.7	-0.00202	0.01001	0.1	0.2%
	0	0	600	39.5	-0.00225	0.01001	39.6	-0.00218	0.01000	0.1	0.2%
	0	0	750	49.4	-0.00235	0.01000	49.5	-0.00229	0.01000	0.1	0.2%
	0	0	900	59.3	-0.00242	0.01000	59.4	-0.00237	0.01001	0.1	0.2%
	0	0	1050	69.2	-0.00247	0.01001	69.3	-0.00242	0.01001	0.1	0.2%
C30	0	0	150	9.6	-0.00109	0.01000	9.6	-0.00100	0.01000	0.0	-0.2%
	0	0	300	19.5	-0.00147	0.01000	19.5	-0.00140	0.01000	0.0	0.0%
	0	0	450	29.4	-0.00172	0.01000	29.4	-0.00166	0.01001	0.0	0.1%
	0	0	600	39.3	-0.00189	0.01000	39.4	-0.00184	0.01001	0.0	0.1%
	0	0	750	49.3	-0.00202	0.01000	49.3	-0.00197	0.01000	0.1	0.1%
	0	0	900	59.2	-0.00211	0.01001	59.2	-0.00208	0.01000	0.1	0.1%
	0	0	1050	69.1	-0.00219	0.01000	69.2	-0.00216	0.01001	0.1	0.1%
C45	0	0	150	9.5	-0.00090	0.01000	9.5	-0.00088	0.01000	0.0	0.0%
	0	0	300	19.3	-0.00124	0.01001	19.3	-0.00123	0.01001	0.0	0.1%
	0	0	450	29.2	-0.00147	0.01000	29.2	-0.00147	0.01001	0.0	0.1%
	0	0	600	39.1	-0.00165	0.01000	39.2	-0.00165	0.01000	0.0	0.1%
	0	0	750	49.1	-0.00178	0.01000	49.1	-0.00178	0.01000	0.0	0.1%
	0	0	900	59.0	-0.00189	0.01000	59.0	-0.00189	0.01001	0.0	0.1%
	0	0	1050	68.9	-0.00198	0.01000	69.0	-0.00198	0.01001	0.0	0.1%

Table 9
Singly-reinforced cross-section subjected to pure bending

	Stress resultants			Parabola-rectangle diagram			Sargin curve			Diff.	Relative difference
	N_x (kN)	M_y (kNm)	M_z (kNm)	$A_{s\,tot}$ (cm²)	$\varepsilon_{c\,min}$	$\varepsilon_{s\,max}$	$A_{s\,tot}$ (cm²)	$\varepsilon_{c\,min}$	$\varepsilon_{s\,max}$	$\Delta A_{s\,tot}$ (cm²)	$\Delta A_{stot}/A_{stot}$
C30	0	0	150	4.8	-0.00126	0.01001	4.8	-0.00113	0.01000	0.0	-0.2%
	0	0	300	9.9	-0.00212	0.01000	9.9	-0.00199	0.01000	0.0	0.0%
	0	0	450	15.3	-0.00317	0.01000	15.4	-0.00286	0.00920	0.0	0.2%
	0	0	600	21.4	-0.00350	0.00710	21.5	-0.00286	0.00568	0.1	0.4%
	0	0	750	28.2	-0.00350	0.00449	28.4	-0.00291	0.00366	0.2	0.6%
	0	0	900	36.1	-0.00350	0.00271	36.4	-0.00281	0.00207	0.3	0.8%
	0	0	1050	70.5	-0.00350	0.00135	74.6	-0.00350	0.00131	4.0	**5.7%**

The examples in Tables 2, 4, and 6, which consider combined compression and bending with smaller eccentricity, yield significant relative differences. A relative difference of -9.0% is found for C15 concrete (Table 4). The negative sign means that the parabola-rectangle diagram is more conservative. C30 and C45 concretes yield relative differences of 13.9% and 28.7%, respectively (Table 6). The positive sign means that the Sargin curve requires more reinforcement. As the absolute differences for C15, C30 and C45 are limited to -1.4 cm², 1.4 cm², and 3.6 cm², respectively, the relative differences are relevant for low reinforcement ratios.

Table 9 investigates reinforcement design in pure bending without compression reinforcement. The concrete class is C30. This analysis demonstrates the good convergence of the proposed method even without any contribution from steel to the stiffness of the compressive block. The relative differences are less than 1% in the first examples, when the tension reinforcement reaches the yield point ($\varepsilon_{smax} \geq 0.00207$). In the last example, the relative difference is 5.7% and the reinforcement strain is below the yield point. ABNT NBR 6118:2014 [10] recommends compression reinforcement in beams to avoid a neutral axis in domain 4. The comparison between the same examples with and without compression reinforcement (Tables 8 and 9) shows that this recommendation also improves the correspondence between the parabola-rectangle and Sargin results in pure bending.

Figure 9 examines an example for the Sargin curve in Table 2 ($e_z = b_z/4$, f_{ck} = 30MPa, and $A_{s\,total}$ = 67.0 cm²). The modulus of the stress resultant vector |S| is plotted as a function of the modulus of the generalized strain vector |k|. The maximum strength value is obtained for |k|=0.00455, which corresponds to $\varepsilon_{c\,min}$ = -0.00308,

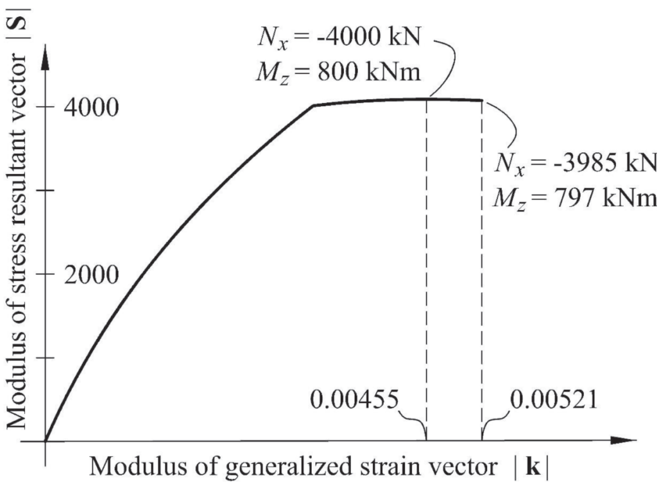

Figure 9
Section under compression and uniaxial bending ($e_z = b_z/4$, f_{ck} = 30 MPa and $A_{s\,tot}$ = 67.0 cm²)

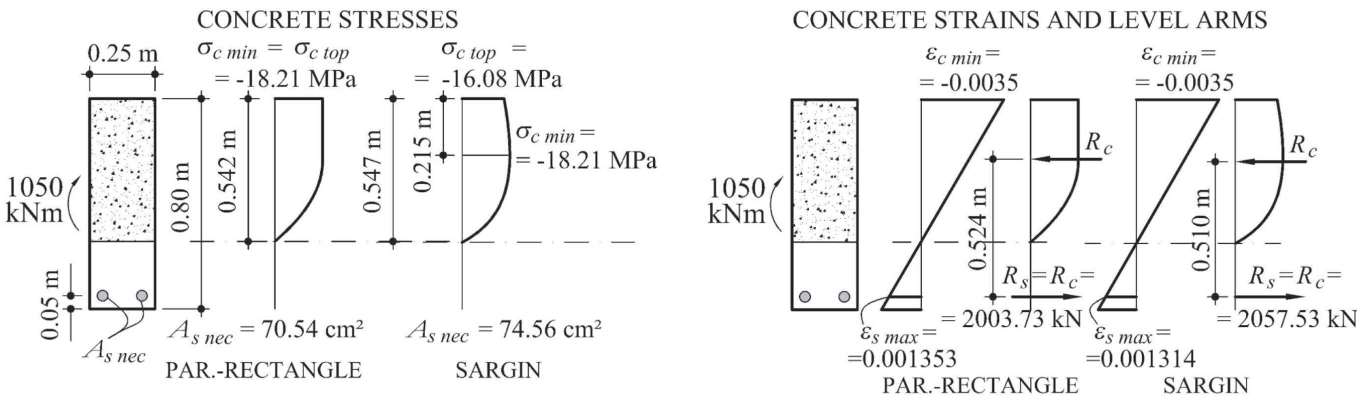

Figure 10
Pure bending without compression reinforcement (M_z = 1050 kNm)

N_x = -4000 kN, and M_z = 800 kNm. However, ultimate concrete strain is reached for |k|=0.00521, which corresponds to $\varepsilon_{c\ min}$ = -0.0035, N_x = -3985 kN, and M_z = 797 kNm.

Figure 10 investigates an example in pure flexion without compression reinforcement (Table 9, M_z = 1050 kNm). The resultants of the compressive stresses in concrete are obtained by numerically integrating the parabola-rectangle and Sargin curves. The required reinforcements are $A_{s\ PAR\text{-}RECT}$ = 70.54 cm² and $A_{s\ SARGIN}$ = 74.56 cm², respectively. The corresponding level arms are $z_{s\ PAR\text{-}RECT}$ = 0.524 m and $z_{s\ SARGIN}$ = 0.510 m, respectively. Reinforcing bars do not reach the yield point in either case. The parabola-rectangle diagram and the Sargin curve yield $\sigma_{c\ topo} = \sigma_{c\ min}$ and $|\sigma_{c\ top}| < |\sigma_{c\ min}|$, respectively, where $\sigma_{c\ top}$ is the stress at the top of the section and $\sigma_{c\ min}$ is the minimum compressive stress in the concrete. The concrete and steel force resultants are $R_c = R_s$ = 2003.73 kN and $R_c = R_s$ = 2057.53 kN for the parabola-rectangle and Sargin curves, respectively.

7. Conclusion

The reinforcement design of concrete sections based on the parabola-rectangle diagram is a practical and well-established model. However, the initial modulus of elasticity and plastic range of the parabola-rectangle diagram do not represent the actual behavior of concrete.

Stress-strain relationships that better characterize concrete properties are needed for global limit analyses of concrete structures that consider their physical and geometric non-linear behavior. The Sargin curve is selected because it is a function of the peak point and initial modulus of elasticity and represents the descending branch of the stress-strain relationship.

This research proposes a numerical procedure for the reinforcement design of concrete sections that uses an arc-length method and yields good convergence in the descending branch of the Sargin curve, without having to consider the distributions of strain limits around pivot C in domain 5. Strain limits for concrete and steel are not required, but they are included in order to avoid excessive deformation. The parabola-rectangle and Sargin curves are considered by using the code provisions for cross-sections and global limit analyses, respectively. The reinforcement design using the parabola-rectangle diagram is based on the section model in ABNT NBR 6118: 2014 [10]. The Sargin curve is implemented according to the global nonlinear model in CEN Eurocode 2: 2004 [8]. The examples consider characteristic concrete strength values of 15, 30, and 45 MPa. The typical 0.25 m × 0.85 m rectangular cross-section is subjected to several loading cases which include pure compression and pure bending. Eccentricities in each direction of 1/4 and 1/2 of the corresponding dimension are considered in uniaxial and biaxial bending.

The required reinforcement shows a good correspondence in pure compression, pure bending of doubly-reinforced cross-sections, and uniaxial and biaxial bending with the highest relative eccentricity. The results also show good correspondence in pure bending of singly-reinforced cross-sections when reinforcing steel reaches the yield point. The comparison of the results shows that the use of compression reinforcement in beams to avoid the neutral axis in domain 4 also improves the correspondence between the results of the parabola-rectangle and Sargin curves.

More significant differences are observed in uniaxial and biaxial bending with the lowest relative eccentricity. The parabola-rectangle diagram is more conservative for C15 concrete, which shows a relative difference of -9.0%. The Sargin curve yields more reinforcement for C30 and C45, which present relative differences of 13.9% and 28.7%, respectively. The relative differences are higher for the lower reinforcement ratios, since the absolute differences are small and limited to -1.4 cm², 1.4 cm², and 3.6 cm² for C15, C30, and C45, respectively.

Despite the good correspondence observed in most examples, the investigation shows that the results of the Sargin curve are not necessarily conservative when compared to the parabola-rectangle diagram. For this reason, a global limit analysis using the Sargin curve still requires the analysis of all cross-sections with the parabola-rectangle diagram.

The proposed reinforcement design method is efficient, numerically robust, and capable of considering other stress-strain relationships with or without descending branches. The examples use local and global analysis parameters for the parabola-rectangle and Sargin curves, respectively. The validation of a single calculation model for section and global limit analyses could motivate future investigations.

8. Acknowledgements

The first author thanks the Coordination for the Improvement of Higher Education Personnel (CAPES) for financial support. The authors thank the valuable suggestions of Prof. Benjamin Ernani Diaz.

9. References

[1] MÖRSCH, E. Concrete-steel construction (Der Eisenbetonbau), The Engineering News Publishing Company, New York, 1910, 368 p.

[2] HOGNESTAD, E. A study of combined bending and axial load in reinforced concrete members, Bulletin Series no. 399, Engineering Experiment Station, University of Illinois, Urbana, 1951, 128 p.

[3] WHITNEY, C. S. Design of reinforced concrete members under flexure or combined flexure and direct compression, ACI Journal, v. 33, n. 1, 1937, p. 483-498.

[4] BITTNER, E. Zur Klärung der n-Frage bei Eisenbetonbalken, Beton und Eisen, 1935, v. 34, n.14, p. 226-228.

[5] MATTOCK, A. H., KRIZ, L. B., AND HOGNESTAD, E. Rectangular concrete stress distribution in ultimate strength design, ACI Journal, 1961, v. 57, n. 2, p. 875-928.

[6] RÜSCH, H., GRASSER, E., AND RAO, P. S. Principes de calcul du béton armé sous états de contraintes monoaxiaux, Bulletin d'Information n. 36, CEB, Paris, 1962, p. 1-112.

[7] AMERICAN CONCRETE INSTITUTE. Building code requirements for structural concrete - ACI 318-14, Farmington Hills, 2015.

[8] COMITÉ EUROPÉEN DE NORMALISATION. Eurocode 2: Design of concrete structures – Part 1-1: General rules and rules for buildings - EN 1992-1-1, Brussels, 2004.

[9] FÉDÉRATION INTERNATIONALE DU BÉTON. FIB Model Code for Concrete Structures 2010, Ernst & Sohn, Berlin, 2013, 402 p.

[10] ASSOCIAÇÃO BRASILEIRA DE NORMAS TÉCNICAS. Projeto de estruturas de concreto –Procedimento – ABNT NBR 6118, Rio de Janeiro, 2014.
[11] SARGIN, M. Stress-strain relationships for concrete and the analysis of structural concrete sections, SM Study n. 4, Solid Mechanics Division, University of Waterloo, Waterloo, Canada, 1971, 167 p.
[12] COMITÉ EURO-INTERNATIONAL DU BÉTON, FÉDÉRATION INTERNATIONALE DE LA PRÉCONTRAINTE. CEB-FIP Model Code 1990, Thomas Telford, London, 1993, 437 p.
[13] RÜSCH, H. Researches toward a general flexural theory of structural concrete. ACI Journal, v. 57, n. 7, 1960, p. 1-28.
[14] CRISFIELD, M. A. A fast incremental/iterative solution procedure that handles "snap-through", Computers & Structures, 1981, v. 13, n. 1-3, p. 55-62.
[15] RIKS, E. An incremental approach to the solution of snapping and buckling problems, International Journal of Solids Structures, 1979, v. 15, n. 7, p. 529-551.
[16] KABENJABU, J. N. Dimensionamento de seções de concreto considerando a curva de Sargin, Niterói, 2017, Dissertation (master's degree) - Dept. Civil Engrg., Federal Fluminense Univ., 196 p. (in Portuguese).